Sequence-Specific ^1H and ^{15}N Resonance Assignments for Both Equilibrium Forms of the Soluble Heme Binding Domain of Rat Ferrocytochrome b_5†

R. D. Guiles,‡,§,‖ Vladimir J. Basus,§ Irwin D. Kuntz,§ and Lucy Waskell*,‡

Departments of Pharmaceutical Chemistry and Anesthesia and The Liver Center, University of California, San Francisco, California 94143, and Anesthesiology Service, Veterans Administration Medical Center, San Francisco, California 94121

Received July 17, 1992; Revised Manuscript Received September 4, 1992

ABSTRACT: ^{15}N and ^1H resonance assignments for backbone and side-chain resonances of both equilibrium forms of rat ferrocytochrome b_5 have been obtained, using ^{15}N–^1H heteronuclear correlation methods employing globally ^{15}N-labeled protein. Unlike other cytochrome b_5 species assigned to date (Guiles et al., 1990) the rat cytochrome exists as an equilibrium distribution of conformers in nearly equal abundance (Lee et al., 1990). The ratio of conformers present in all other species variants is approximately 1:9. More than 40% of all residues of the rat protein exhibit NMR-detectable heterogeneity due to the 180° rotation of the heme about the α,γ-meso axis. NOESY and HOHAHA relayed ^{15}N–^1H double-DEPT heteronuclear correlation methods were an indispensible tool for the deconvolution of a system with this level of heterogeneity. Differences in the resonance assignments between the two equilibrium conformers were found to be as great as differences between species variants we have previously reported. On the basis of the magnitude and extent of the observed chemical shift differences and specific NOESY connectivities observed in the two isomers, we believe the two equilibrium conformers differ not only by a simple back-to-front flip of the heme but also by an additional rotation about an axis normal to the heme plane as has been previously suggested by Pochapsky et al. (1990). A short segment of the protein at the N-terminus could not be assigned, presumably due to rapid exchange of solvent-accessible amide protons in this disordered segment of the protein. Assignments for 93 of the 98 residues of this 12-kDa protein have been obtained.

Long-range interprotein electron-transfer reactions are at the core of cellular bioenergetic processes. The fundamental importance of this class of reactions has stimulated a great deal of experimental and theoretical work. The pioneering work of Gray and co-workers has yielded much insight into intramolecular electron-transfer rates of structurally well-characterized, chemically derivatized model protein systems [for reviews see Gray and Malmstrom (1989), Mayo et al. (1986), and Scott et al. (1985)]. As a result of this work significant progress is being made toward a better theoretical understanding of the details of protein structure which control rates of electron transfer (Beretan et al., 1990a,b). Much less progress has been made toward an understanding of the details of molecular recognition in interprotein electron-transfer events, principally due to a lack of structurally well-characterized systems.

A number of small protein complexes have been studied theoretically [e.g., cytochrome b_5–cytochrome c, Salemme (1976); cytochrome c–cytochrome c peroxidase, Poulos and Kraut (1980); cytochrome b_5–hemoglobin, Poulos and Mauk (1983)]. The cytochrome b_5–cytochrome c complex has been the most extensively studied (Wendoloski et al., 1987). Docking calculations employing high-resolution X-ray crystal structures of the component proteins have optimized surface and charge complementarity. The principal basis of these studies has been chemical modification (Ng et al., 1977) or more recently site-directed mutagenesis studies of the complex (Rodgers et al, 1988; Rodgers & Sligar, 1991). These experimental studies clearly indicate which charged residues on each protein are involved in docking, but they cannot establish specific interprotein contacts. For example, it is known through mutational studies that the carboxyl of Glu-44 is one of the negatively charged groups of cytochrome b_5 involved in interprotein salt bridges with cytochrome c. However, there is no direct experimental evidence indicating which specific positively charged group on cytochrome c interacts directly with Glu-44. The docking studies implicate Lys-27 on cytochrome c. Attempts to characterize such protein complexes crystallographically have to date been unsuccessful (Poulos et al., 1987).

Our interest in the solution structure of cytochrome b_5 has in large measure been motivated by a desire to obtain direct experimental evidence relating to the structure of the cytochrome b_5–cytochrome c complex in solution. We have recently performed a number of ^{15}N-filtered NMR[1] studies of the cytochrome c–^{15}N-labeled cytochrome b_5 complex which are promising in this regard. These results will be published in a separate report.

† Supported by National Institutes of Health Grants GM 35533 (L.W.), GM 19267 (I.D.K.), and RR 1695 (I.D.K.) and by a Veterans Administration Merit Review (L.W.). The UCSF Magnetic Resonance Laboratory was partially funded by grants from the National Science Foundation (DMB 8406826) and the National Institutes of Health (RR 01668).

* Correspondence should be addressed to this author at the Veterans Administration Medical Center, Department of Anesthesia (129), 4150 Clement St., San Francisco, CA 94121.

‡ Department of Anesthesia and The Liver Center.

§ Department of Pharmaceutical Chemistry.

‖ Present address: Department of Biomedicinal Chemistry, School of Pharmacy, University of Maryland at Baltimore, 20 North Pine St., Baltimore, MD 21201.

[1] Abbreviations: NMR, nuclear magnetic resonance; TSP, sodium-(trimethylsilyl)propionate; NOE, nuclear Overhauser effect; NOESY, 2D NOE spectroscopy; COSY, 2D correlated spectroscopy; HMQC, 2D heteronuclear multiple quantum correlation spectroscopy; HOHAHA, 2D homonuclear Hartman–Hahn spectroscopy; DEPT, distortionless enhancement of polarization transfer; double-DEPT, 2D heteronuclear correlation employing DEPT and reverse DEPT sequences, t_1, evolution time; t_2, data acquisition time; ω_1, Fourier transformed t_1 data; ω_2, Fourier transformed t_2 data; ppm, parts per million.

0006-2960/92/0431-11365$03.00/0

Herein we report the ^{15}N and proton resonance assignments for 93 of the 98 residues of the structured domains of both equilibrium forms of the soluble heme binding domain of rat ferrocytochrome b_5 obtained by bacterial expression of the synthetic gene (von Bodman et al., 1986). This soluble synthetic gene product differs substantially form the trypsin-solubilized bovine, porcine, or rabbit proteins we have previously characterized (Guiles et al., 1990) in a number of respects. It is significantly larger than the tryptic fragments, having 6 and 10 amino acid extensions at the amino and carboxyl termini, respectively. This 98-residue protein is about 12 kDa while the tryptically solubilized microsomal proteins are 82 residues and about 10 kDa. There are 6 and 8 differences in the amino acid sequence between the rat and porcine or bovine proteins, respectively. The presence of a valine at position 23 in the rat protein instead of the isoleucine present in most other species variants has a profound effect on the equilibrium distribution of conformers in solution (Lee et al., 1990). The equilibrium distribution of heme orientations changes from about 1:9 in the bovine, porcine, and rabbit proteins to close to 60:40 for the rat protein under the conditions described in this work.

Because of their reasonably small size, high solubility, and large proton dispersion, cytochromes have been extensively studied using NMR methods. Although several have been fully assigned (Wand et al., 1989; Detlefsen et al., 1990; Gooley et al., 1990), some like cytochrome b_5 in more than one oxidation state (Feng et al., 1989; Veitch et al., 1990), only recently has the solution structure of a cytochrome been determined using NMR methods (Detlefsen et al., 1991). Although a solution structure of cytochrome b_5 has not been determined, some of the earliest studies of the protein clearly demonstrated the extreme sensitivity of NMR methods to subtle details of protein structure. One of the first NMR studies (Keller & Wüthrich, 1980) clearly showed that the original crystal structure (Mathews et al., 1972) depicted what is now known to be the lower abundance orientation of the heme in the bovine protein. There is now an abundance of experimental evidence supporting the existence of a slow equilibrium between two forms of the protein which differ by a 180° rotation of the heme about the α,γ-meso axis. Evidence presented in this article and previously suggested by Pochapsky et al. (1990) indicates that additional differences in the binding of the heme to the protein in each conformation also exist. Detailed structural calculations are currently underway which should clearly elucidate differences in the interactions of the heme with the protein in each conformational isomer which mediate differences in the physical properties such as midpoint potential. We believe the elucidation of these subtle differences represent an interesting test of the resolution of current NMR solution structure methods.

MATERIALS AND METHODS

Rat Cytochrome b_5: Preparation and Labeling. Unlabeled rat cytochrome b_5 holoprotein was isolated from *Escherichia coli* strain TB-1 harboring a pUC13 plasmid containing the synthetic gene coding for the 98 amino acid polypeptide corresponding to the soluble portion of rat cytochrome b_5 (von Bodman et al., 1986). The plasmid was generously provided by Dr. S. G. Sligar. The bacteria were grown at 37 °C in rich culture media (10 g/L yeast extract, 10 g/L bactotryptone, and 10 g/L NaCl). Cytochrome b_5 was isolated using a minor modification of the published procedure (von Bodman et al., 1986). Uniformly ^{15}N-enriched (>99%) protein was obtained by growth of *E. coli* on M9 minimal media (McIntosh et al., 1987) containing glycerol as a carbon source and $^{15}NH_4Cl$ as the sole source of nitrogen. Expression of the protein in minimal media was found to vary significantly as a function of the host strain of *E. coli*. We found a 20-fold increase in expression on changing host strain from the *E. coli* K-12 host TB-1 to NCM 533, a strain obtained from the laboratory of Dr. H. Boyer at UCSF. Unlike the TB-1 host strain (r^+, m^- derivative of JM83; T. O. Baldwin, Texas A&M; also distributed by Bethesda Research Laboratories) the NCM 533 strain (geneotype lacZ:TN5,lacI^{Q1},λ^+) is an overproducer of the *lac* repressor and is not a proline auxotroph (Shand et al., 1991). Expression of the protein was induced by addition of 1 mM IPTG. We obtained 37 mg of purified ^{15}N-labeled cytochrome b_5 from a 12-L culture.

Electrospray mass spectrometry of both the ^{15}N-enriched and natural abundance proteins indicated that the labeled protein was enriched to greater than 99.7% in ^{15}N. On the basis of the molecular weight determined (e.g., 11 210.1 ± 0.3), we found that the N-terminal methionine coded by the synthetic gene had been posttranscriptionally cleaved. Also a proteolytic product at about the 10% level was detected. This product corresponded to cleavage between K86 and I87.

NMR Sample Preparation. The purified proteins were desalted over a coarse G-25 column and lyophilized from a 100 mM ammonium bicarbonate solution. The lyophilized cytochrome b_5 samples were dissolved in 100 mM pH 7 phosphate buffers prepared in either 90% H_2O (10% D_2O) or 99.96% D_2O. Cytochrome b_5 samples prepared in 99.96% D_2O buffers were lyophilized twice from 99.96% D_2O prior to dissolution in the final 100 mM phosphate buffer. Small adjustments in the pD to a final value of 7.0 were made by additions of small aliquots of 0.25 M NaOD or DCl. Measurements of pH were not corrected for isotope effects. (Trimethylsilyl)propionic acid (TSP) was added to a final concentration of 1 mM as an internal chemical shift reference. Cytochrome b_5 solutions were reduced by addition of a small quantity of solid sodium dithionite. The protein solutions were purged with argon prior to the addition of the sodium dithionite, and then the NMR tubes were sealed under vacuum using a gas–oxygen torch. Cytochrome b_5 concentrations between 5 and 7 mM were used in all NMR experiments. Concentrations of the ferric protein were determined using an absorption coefficient of 117 mM^{-1} at 413 nm (Strittmatter & Velick, 1956).

Two-Dimensional NMR Spectra. NMR spectra were recorded on a 500-MHz General Electric GN-500 NMR spectrometer. All spectra were recorded in phase-sensitive mode with quadrature detection in both dimensions using a spectral width of 7246 Hz for protons. ^{15}N spectra were recorded with a spectral width of 5000 Hz. All two-dimensional spectra were recorded at 40 °C. Relaxation delay times of 3.5 s were used in all cases. NOESY spectra were acquired using the method of States et al. (1982). Mixing times of 100 and 200 ms were used. Water suppression for H_2O NOESY spectra was accomplished by continuous-wave preirradiation or by an inversion–recovery sequence coupled with a jump–return read sequence (Basus, 1984). Double-quantum-filtered COSY (Piantini et al., 1982; Shaka & Freeman, 1983) spectra were acquired using time-proportional phase incrementation of the first pulse (Redfield & Kunz, 1975). HOHAHA spectra using the MLEV-17 spin lock sequence (Bax & Davis, 1985) were acquired using a transmitter equipped with a 6-W high-power amplifier. Mixing times of 50, 70, and 100 ms were used. Water suppression in the HOHAHA experiment in H_2O was achieved

using a DANTE sequence. DQFCOSY were acquired with 1024 t_1 increments and were zero filled to 1024 data points with 4096 points in ω_2. All other spectra were acquired with 512 t_1 and zero filled in t_1 to give a real matrix of 1024 points by 2048 points in ω_2. All spectra were recorded with a spectral width of 7246 Hz.

Double-DEPT sequences (Nirmala & Wagner, 1988) were used in the acquisition of ^{15}N proton heteronuclear correlation experiments or NOESY and HOHAHA relayed heteronuclear correlation experiments. Heteronuclear multiple quantum coherence (HMQC) spectra (Bax et al., 1983) and COSY relayed HMQC spectra (Gronenborn et al., 1989) were also recorded using samples of the ^{15}N-labeled protein. Our experience with the double-DEPT experiment indicates a somewhat lower sensitivity than the HMQC experiment but better resolution especially for correlation peaks of residues in the β-sheet regions of the protein, due to secondary amide proton couplings seen in the HMQC experiment. Nitrogen-15 chemical shifts are referenced to an external $^{15}NH_4Cl$ reference standard obtained from Wilmad Corp. (WGN-01) and are reported relative to liquid ammonia. The center of the ^{15}N spectrum was set at the ^{15}N frequency of the D82 amide nitrogen which is about 128 ppm downfield from liquid ammonia. All heteronuclear correlation spectra were recorded with broad-band heteronuclear decoupling using the WALTZ-16 sequence (Shaka et al., 1983) during proton detection.

Data Analysis. Two-dimensional NMR spectra were transfered to Spark workstations (Sun Microsystems, Mountainview, CA) running a UNIX operating system (SunOS 4.1.1). Two-dimensional NMR spectra were processed using software originally developed in the laboratory of Dr. Kaptein at the University of Groningen, Groningen, The Netherlands. Many modifications and improvements have been made by Dr. R. M. Scheek, Dr. S. Manogaran, and Mr. M. Day and Dr. D. Kneller in our laboratory. For all double-quantum-filtered COSY experiments a 70° phase-shifted sine-squared bell was applied. For NOESY and HOHAHA and heteronuclear correlation spectra, Gaussian filters with line-broadening parameters of 6–8 Hz were used. Automatic baseline correction of H_2O spectra was accomplished by an adaptation of an algorithm originally described by Pearson (1977).

RESULTS

The work presented here is a significant extension over our previous cytochrome b_5 assignments (Guiles et al., 1990) in that we have now obtained nearly complete ^{15}N and proton resonance assignments for the rat cytochrome containing both equilibrium conformations of the heme (see Table I). This was only possible because the 60/40 equilibrium ratio of conformers in the rat protein is significantly altered from the 1:9 ratio observed in the porcine, bovine, and rabbit species variants. While this reduced the sensitivity of measurements that could be made on each isomer, it enabled unambiguous assignment of the lower abundance form [herein referred to as the B-isomer—nomenclature used by Pochapsky et al. (1990)]. Of course, the doubling of numerous spin systems also complicated the total assignment problem. The expression product of the synthetic gene coding for the rat protein (ca. 12 kDa) is also significantly larger than the tryptic fragments of the other species variants (ca. 10 kDa) we have previously assigned. Given the increased size of the protein and the more pronounced heterogeneity observed, it would have been impossible to assign the rat protein by proton methods alone.

Assignment Approach. Heteronuclear correlation methods were essential to establishing unique assignments specific both to the sequence and to each equilibrium conformer, due to the superior sensitivity (i.e., compared to homonuclear methods), the conformationally independent peak intensities, and the high dispersion of the ^{15}N amide resonances. Assignment of the major abundance conformer was facilitated by detailed comparisons with other species variants which we have previously assigned (Guiles et al., 1990). Given the similarity of the heme orientation and the primary sequence, it is perhaps not surprising that the porcine assignments most closely resemble the major abundance conformer (isomer A) of the rat protein. However, direct transfer of assignments was seriously complicated by ambiguities introduced by the significantly increased complexity of the spectra and due to large differences in chemical shifts between the rat protein and all other species variants. The origin of the heterogeneity is due to a 180° rotation about the α,γ-meso axis of the heme. Thus, conformation-specific assignments can only be made based on heme proton to protein proton NOESY connectivities which are unique to each isomer. However, given the known ratio of isomer abundances, we have found that heteronuclear correlation peak intensities can provide corroborative evidence of specific isomer assignments.

Side-chain assignments were carried out with methods patterned after those developed by Wüthrich and coworkers (Wüthrich et al., 1984; Billeter et al., 1982). As in our previous work, HOHAHA experiments in conjunction with double-quantum-filtered COSY experiments were an indispensible tool for delineating many amino acid spin systems. Here again, however, assignment of sequence-specific and isomer-specific side-chain resonances was facilitated by examination of HOHAHA relayed heteronuclear correlation spectra. Sequence-specific and conformer-specific assignments were greatly facilitated by NOESY relayed heteronuclear correlation spectra. Assignment of side chains did not proceed independent of sequence-specific assignments. Often, through an analysis of both conventional NOESY spectra and NOESY relayed heteronuclear correlation spectra, a series of unambiguous sequential assignments could be made in parallel for both equilibrium conformers from residues with well-defined side chains. The preponderance of ill-defined AMX spin systems in cytochrome b_5 necessitates this approach. Ultimately, complete assignment was achieved through the analysis of nine spectra (a ^{15}N–^1H correlation spectrum, a HOHAHA relayed ^{15}N–^1H correlation spectrum, a NOESY relayed ^{15}N-^1H correlation spectrum and double-quantum-filtered COSY spectra, ^1H–^1H NOESY and HOHAHA spectra recorded in both H_2O and D_2O). In parallel, we have been examining spectra of rat ferricytochrome b_5. In some cases spectral simplification due to line broadening or the increased dispersion due to pseudocontact effects were an aid in deconvoluting dense regions of the diamagnetic protein.

Table I contains a nearly complete list of ^{15}N and ^1H assignments for both forms of the rat protein. Note that we were unable to assign a short segment (5 residues) of amino acids on the N-terminal side of the protein up to D1. We believe this is due to a lack of well-defined secondary structure for this part of the protein and the high pH (pH 7) used in all experiments which presumably resulted in rapid exchange of solvent-exposed amide protons. The X-ray crystal structure of the lipase-solubilized bovine cytochrome b_5 (Mathews et al., 1972) provides some corroborative support for this hypothesis in that electron density was not observed for residues 1 and 2 presumably due to disorder in the crystal at these positions. Similar difficulties in the assignment of unstructured N-terminal domains of proteins have previously been reported

Table I: Summary of Sequence-Specific Proton and ^{15}N Resonance Assignments for Rat Cytochrome b_5[a]

residue[b]	^{15}N	NH	$C^{\alpha}H$	$C^{\beta}H$	$C^{\beta'}H$	other assignments	residue[b]	^{15}N	NH	$C^{\alpha}H$	$C^{\beta}H$	$C^{\beta'}H$	other assignments
D1	124.8	8.37	4.62	2.69	2.02		A50(B)	127.7	7.21	4.27	1.69		
K2	127.0	8.04	4.30	1.76		1.41 (γ), 1.66 (δ)	G51(A)	116.3	9.69	4.05			3.82 (α')
D3	124.3	8.19	4.60	2.68	2.57		G51(B)	115.7	9.67	4.04			3.82 (α')
V4	127.6	7.63	3.87	1.65		0.70 (γ), 0.40 (δ)	G52(A)	111.5	7.79	4.47			3.92 (α')
K5	133.3	8.07	4.16	1.65		1.44 (γ), 2.95 (ϵ)	G52(B)	111.1	7.65	4.43			3.95 (α')
Y6	128.1	8.12	5.74	2.89	2.68	6.92 (δ), 6.66 (ϵ)	D53(A)	124.1	8.62	5.25	3.07	2.49	
Y7	124.9	8.73	5.23	3.23	2.55	6.98 (δ), 6.64 (ϵ)	D53(B)	123.9	8.66	5.23	3.02	2.49	
T8	121.6	9.19	4.67	4.90		1.26 (γ)	A54(A)	136.8	9.24	5.24	1.75		
L9	130.3	9.75	4.12	1.60		1.77 (γ), 1.06 (δ), 1.00 (δ')	A54(B)	137.8	9.26	5.26	1.87		
E10	123.6	8.44	3.99	2.07	2.00	3.26 (γ)	T55(A)	124.1	8.44	3.38	4.10		0.47 (γ)
E11	124.9	7.69	4.12	2.33	2.19	2.51 (γ)	T55(B)	124.0	8.41	3.33	4.10		0.45 (γ)
I12	128.0	8.52	3.79	2.03		1.35 (γ), 1.59 (γ'), 1.02 (γCH_3), 0.97 (δ)	E56(A)	125.8	8.79	3.90	2.23	1.99	2.31 (γ)
Q13	121.8	8.22	4.38	2.25	2.03	2.67 (γ)	E56(B)	125.8	8.73	3.87	2.23	2.00	2.29 (γ)
K14	121.9	7.32	4.12	1.67		1.45 (γ), 1.62 (δ), 2.98 (ϵ)	N57(A)	123.3	7.93	4.43	2.82	2.67	
H15	128.0	7.73	4.18	2.48	2.17	6.85 (δ), 8.00 (ϵ)	N57(B)	123.6	7.92	4.42	2.85	2.67	
K16	123.5	7.46	4.84	1.80		1.33 (γ), 1.79 (δ), 3.13 (ϵ)	F58(A)	126.0	8.66	3.84	2.87		
D17	128.0	8.07	4.91	3.08	2.63		F58(B)	126.1	8.73	3.87	2.87		
S18	121.8	7.39	4.49	3.96			E59(A)	124.8	8.32	3.83	1.89		2.69 (γ)
K19	126.0	8.02	4.23	1.86		1.42 (γ'), 1.65 (δ), 2.97 (ϵ)	E59(B)	124.8	8.38	3.83	1.89		2.70 (γ)
S20	119.4	7.44	5.00	3.87	3.77		D60(A)	127.8	8.20	4.23	2.79	2.58	
T21	129.1	8.65	4.53	3.64		1.00 (γ)	D60(B)	127.5	8.22	4.23	2.79	2.58	
W22(A)	133.4	8.76	6.53	3.23	3.05	6.78 (ϵ_3), 5.93 (ζ_3), 6.50 (η_2), 6.76 (ζ_2), 8.90 ($N\epsilon_1$), 131.4 ($^{15}N\epsilon$)	V61(A)	122.8	6.73	3.30	0.40		0.78 (γ), −1.07 (γ')
W22(B)	133.3	8.78	6.55	3.24	3.05	6.78 (ϵ_3), 5.94 (ζ_3), 6.53 (η^2), 6.79 (ζ_2), 8.90 ($N\epsilon_1$), 131.4 ($^{15}N\epsilon$)	V61(B)	122.9	6.57	3.25	0.22		0.79 (γ), −1.19 (γ')
V23(A)	119.8	8.98	5.12	2.33		1.13 (γ), 1.05 (γ')	G62	112.0	6.56	3.42			3.23 (α')
V23(B)	120.2	8.97	5.12	2.39		1.16 (γ), 1.06 (γ')	H63(A)	122.9	6.02	2.59	0.37		0.23 (δ), 0.76 (ϵ)
I24(A)	129.2	8.50	5.49	1.69			H63(B)	122.8	5.96	2.58	0.33		0.35 (δ), 0.74 (ϵ)
I24(B)	129.1	8.39	5.51	1.78			S64(A)	128.7	9.71	4.07	4.27		
L25(A)	130.5	8.99	4.93	1.87		1.18 (γ), 0.57 (δ), −0.37 (δ')	S64(B)	128.7	9.69	4.07	4.27		
L25(B)	129.3	8.96	4.91	1.85		1.13 (γ), 0.64 (δ), −0.49 (δ')	T65	125.8	8.72	3.83	4.23		1.28 (γ)
H26	131.3	9.52	4.02	3.23		7.01 (δ), 8.92 (ϵ)	D66(A)	127.8	7.97	4.50	2.86		
H27	114.6	8.77	4.06	2.95		7.04 (δ), 8.09 (ϵ)	D66(B)	127.8	7.94	4.49	2.86		
K28(A)	128.5	8.46	4.96	2.33		1.61 (γ), 1.52 (δ), 3.07 (ϵ)	A67(A)	131.7	8.54	4.74	1.23		
K28(B)	128.4	8.41	4.96	2.33		1.61 (γ), 1.52 (δ), 3.07 (ϵ)	A67(B)	131.7	8.56	4.74	1.23		
V29	127.6	8.49	4.49	1.26		0.77 (γ), 0.30 (γ)	R68(A)	123.8	8.09	3.67	1.78		
Y30(A)	133.3	9.26	4.90	3.00		7.23 (δ), 6.91 (ϵ)	R68(B)	123.5	8.01	3.67	1.78		
Y30(B)	133.3	9.26	4.87	3.08		7.14 (δ), 6.84 (ϵ)	E69(A)	129.2	8.62	4.17	2.51		2.44 (γ)
D31	126.5	8.35	5.23	3.05	2.55		E69(B)	128.9	8.69	4.17	2.51		2.44 (γ)
L32	129.9	8.77	4.07	1.82		1.92 (γ), 1.15 (δ), 1.02 (δ')	L70(A)	129.3	8.39	4.44	2.69	2.03	1.74 (γ), 0.91 (δ), 0.69 (δ')
T33	128.5	8.63	3.56	4.27		1.33 (γ)	L70(B)	129.3	8.47	4.46	2.69	2.01	1.69 (γ), 0.91 (δ), 0.67 (δ')
K34(A)	123.4	8.98	4.30	1.87		1.42 (γ), 1.70 (δ), 3.02 (ϵ)	S71(A)	120.7	8.65	4.20	3.96		
K34(B)	123.5	9.12	4.28	1.90		1.42 (γ), 1.70 (δ), 3.02 (ϵ)	S71(B)	120.8	8.62	4.20	3.96		
F35(A)	126.1	7.71	4.43	2.40	1.98	6.56 (δ), 6.32 (ζ), 7.12 (ϵ)	K72(A)	127.0	7.34	4.22	2.02		1.80 (γ), 1.62 (δ), 3.06 (ϵ)
F35(B)	125.9	7.69	4.37	2.37	2.12	6.55 (δ), 6.23 (ζ), 6.97 (ϵ)	K72(B)	127.4	7.43	4.23	2.02		1.80 (γ), 1.62 (δ), 3.06 (ϵ)
L36(A)	124.4	7.02	2.95	1.57		1.76 (γ), 0.79 (δ), 0.51 (δ')	T73(A)	117.9	7.94	3.99	3.84		0.94 (γ)
L36(B)	124.1	6.94	2.98	1.59		1.80 (γ), 0.82 (δ), 0.53 (δ')	T73(B)	118.5	7.90	4.02	3.92		0.96 (γ)
E37(A)	117.7	7.62	3.78	1.89	1.77	2.07 (γ)	Y74(A)	124.6	7.72	4.73	2.83		7.21 (δ), 6.46 (ϵ)
E37(B)	117.6	7.67	3.78	1.88	1.76	2.07 (γ)	Y74(B)	124.6	7.77	4.72	2.77		7.27 (δ), 6.57 (ϵ)
E38	123.1	7.02	4.02	2.07	1.64		I75	127.4	6.98	3.67	1.59		0.95 (δ), 0.87 (γCH_3), 0.08 (γ)
H39(A)	126.1	6.01	2.45	0.82	0.41		I76	126.0	8.84	4.68	1.92		0.12 (γ), 0.32 (γ'), 0.82 (γCH_3), −1.00 (δ)
H39(B)	126.7	5.91	2.52	0.87	0.56		G77	117.0	7.47	4.48			4.18 (α')
P40		NA	3.58	1.63		1.67 (γ), 3.74 (δ), 1.28 (δ')	E78	125.6	9.10	5.24	1.84		2.27 (γ)
G41	113.1	6.13	3.37			0.37 (α')	L79	124.9	8.72	4.37	1.99		2.32 (γ), 1.06 (δ), 1.01 (δ')
G42	113.1	6.15	3.95			3.40 (α')	H80	137.0	9.07	3.84	2.66		7.02 (δ), 7.66 (ϵ)
E43(A)	127.5	8.16	3.59	1.74	1.62	1.89 (γ)	P81		NA	3.80	2.04		1.63 (γ), 2.67 (δ), 2.36 (δ')
E43(B)	124.5	8.15	3.58	1.73	1.65	1.91 (γ)	D82	127.8	10.98	4.52	2.72		
E44(A)	128.3	8.32	3.72	1.95		2.27 (γ)	D83	124.3	8.22	4.98	2.76		
E44(B)	128.3	8.37	3.73	1.95		2.27 (γ)	R84	126.4	7.43	4.04	1.82		1.59 (γ), 2.95 (δ)
V45(A)	119.5	8.25	4.12	2.55		0.99 (γ), 0.91 (γ')	S85	131.6	7.78	3.77	3.89		
V45(B)	119.1	8.18	4.16	2.56		0.97 (γ), 0.87 (γ')	K86	127.4	7.70	4.33	2.02	1.97	1.59 (γ), 3.10 (ϵ)
L46(A)	123.1	6.01	3.90	1.50	0.62	0.26 (γ), −0.69 (δ), −0.72 (δ')	I87	122.1	7.37	4.37	2.12		1.02 (γ), 1.37 (δ)
L46(B)	123.8	6.13	3.92	1.49	0.62	0.25 (γ), −0.60 (δ), −0.80 (δ')	A88	127.4	7.87	4.42	1.44		
R47(A)	124.7	7.97	3.78	1.79		1.49 (γ), 3.07 (δ)	K89	128.7	8.27	4.67	1.76		1.55 (γ), 1.53 (γ')
R47(B)	124.8	7.92	3.78	1.79		1.49 (γ), 3.07 (δ)	P90						
E48(A)	123.3	8.07	4.12	2.37	2.19	2.50 (γ)	S91		8.69	3.76	3.36		
E48(B)	123.0	8.02	4.12	2.37	2.20	2.48 (γ)	E92	131.6	7.76	4.18	1.62	1.49	2.80 (γ)
Q49(A)	120.3	7.17	4.60	1.99		2.76 (γ)	T93	121.9	8.13	4.38	4.25		1.22 (γ)
Q49(B)	120.4	7.27	4.59	2.01		2.76 (γ)	L94	137.1	7.85	4.22	1.62		1.62 (γ), 0.92 (δ), 0.87 (δ')
A50(A)	127.7	7.22	4.28	1.70									

[a] Proton chemical shifts are referenced to TSP, and ^{15}N chemical shifts are reported relative to ammonia. [b] Amino acid sequences taken from von Bodman et al. (1986). When separate conformation-specific resonances could be unambiguously assigned, the letters A and B are used to specify the particular conformation. The amino acids are referred to by their single-letter symbols.

(Torchia et al., 1989). Table I contains more than 740 resonance assignments. This is approaching twice the number of assignments we reported for the bovine protein (Guiles et al., 1990). As indicated above, this increased complexity is due to two factors: (1) widespread doubling of peaks due to the nearly equally abundant heme orientations and (2) the larger size of the rat protein.

Advantages of Heteronuclear Correlation Methods in the Assignment of Rat Cytochrome b_5. The advantages of heteronuclear correlation methods in the assignment of proteins

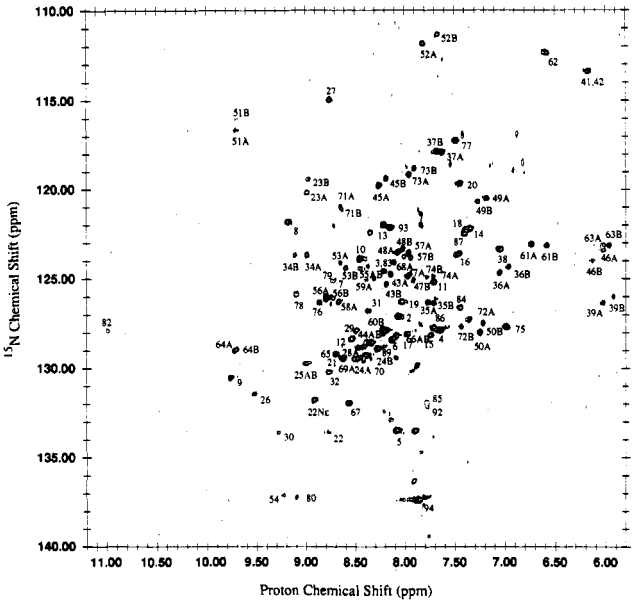

FIGURE 1: Contour plot of the fingerprint region of a 500-MHz ^{1}H–^{15}N heteronuclear correlation spectrum of 7 mM ^{15}N-labeled rat cytochrome b_5 recorded in 90% H_2O/10% D_2O at pH 7.0 (100 mM phosphate buffer) and 40 °C using the double-DEPT sequence. The one-bond correlation peaks between the amide ^{15}N and the amide proton are labeled for all assigned amino acids. For nearly 40% of the protein two distinct correlation peaks are observed due to the two orientations of the heme. These peaks are labeled A and B corresponding to the major and minor abundance conformers of the heme which exist in a 60/40 ratio under the conditions of the experiment. The Trp-22 indole ^{15}N-proton correlation peak is also labeled in the spectrum. Side-chain amide correlation peaks have been largely suppressed due to the selective nature of the DEPT sequence which edits out AX_2 spin system by setting the θ pulse equal to 90°.

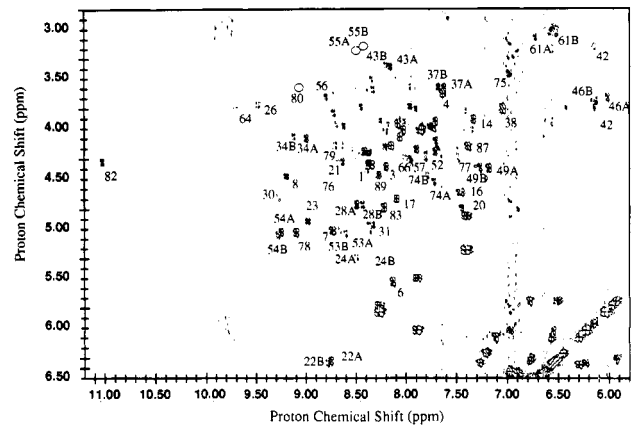

FIGURE 2: Contour plot of the fingerprint region of a double-quantum-filtered COSY spectrum of 7 mM rat cytochrome b_5 recorded in H_2O at 40 °C. The C$^\alpha$H–NH cross-peaks are labeled with sequence-specific assignments. Correlation peaks corresponding to major (A) and minor (B) abundance conformers are labeled accordingly in the figure. Circles are used to clarify the posititons of a few weak peaks or to indicate the postions of peaks determined from other spectra. For the sake of clarity the dense cluster of correlation peaks centered at about 8.25 ppm along ω_2 and 4.00 along ω_1 are labeled on an expanded scale in Figure 3.

are now well established [for a review, see Bax (1989) and Griffey and Redfield (1987)]. Several advantages of heteronuclear methods over proton methods in the assignment of rat cytochrome b_5 can be clearly seen from a comparison of Figures 1 and 2. First, the sensitivity of heteronuclear correlation spectra is a great deal better than that of homonuclear double-quantum-filtered COSY spectra due principally to the much larger one-bond coupling constants between ^{15}N and the

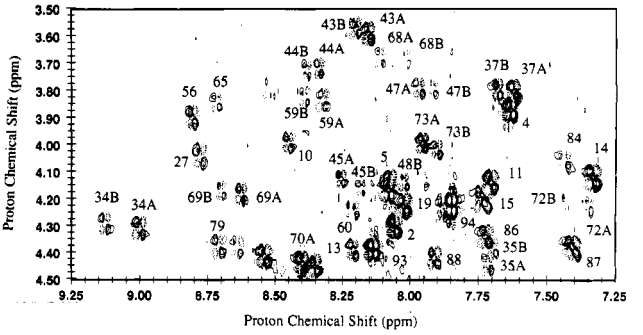

FIGURE 3: Contour plot of a small segment of the fingerprint region of a double-quantum-filtered COSY of rat cytochrome b_5. The sample and spectrometer conditions are identical to those of Figure 2. C$^\alpha$H–NH cross-peaks are labeled with conformer-specific assignments as described in Figure 2. The high density of peaks in this region is due in part to the widespread doubling of peaks due to the conformational heterogeneity and due to the lower dispersion of amide resonances for helical residues.

attached proton. Second, the reliability of the heteronuclear correlation spectra is better than that of COSY spectra. Virtually all expected correlations for both conformations of the protein are present in the heteronuclear correlation spectrum due to the large nearly uniform one-bond ^{15}N–^{1}H coupling constant (~90 Hz). Conversely, the intensity of the COSY peaks varies widely, and as we found previously, cross-peaks may be completely missing due to unusually small $^3J_{N\alpha}$ couplings. In this sense, the present work both extends and validates our previous assignments. Where, previously, we had to rely on indirect methods using NOESY cross-peaks where fingerprint COSY peaks were missing, here intense, well-resolved heteronuclear correlation peaks clearly define amide chemical shifts. A number of fingerprint peaks which are missing from the DQFCOSY in Figure 2 due to near-zero $^3J_{N\alpha}$ couplings are indicated by circles. Third, the high dispersion of ^{15}N resonances allows resolution of all individual resonances associated with each amino acid while there are sections of the fingerprint region of the DQFCOSY in Figure 2 that are so dense that all individual peaks could not be easily labeled on the same scale. The dispersion in the ^{15}N dimension is as high as the dispersion of the amide proton resonances which is anomalously high in heme proteins. Also as described below, the sensitivity of ^{15}N resonances to subtle changes in chemical environment is higher. In addition, as described in detail below, the conformationally independent peak intensities were useful in determining heme conformation-specific assignments.

A Comparison of Resonance Assignments for the Conformers of the Rat Protein. For many amino acids, side-chain heterogeneity was more marked than that observed in the main-chain proton resonances. Perhaps not surprisingly, hydrophobic side chains forming the heme-binding pocket often showed large shifts as is illustrated in Figure 4. In some cases, such as Y30, only side-chain heterogeneity is observed. It is interesting to note that the aromatic ring of Y30 is not in direct contact with the heme. It is, however, plausible that the observed shifts in the resonance frequencies of the aromatic ring are mediated by shifts in the L25 δ-methyl proton positions inducing long-range ring-current effects due to the heme. A number of aromatic and aliphatic side-chain resonances of residues in the heme-binding pocket have recently been assigned, largely on the basis of one-dimensional NOE measurements from the known heme protons (Pochapsky et al., 1990). Our assignments largely agree with those reported, except for minor differences due to the temperatures at which spectra were recorded (e.g., 25 °C vs 40 °C in this study).

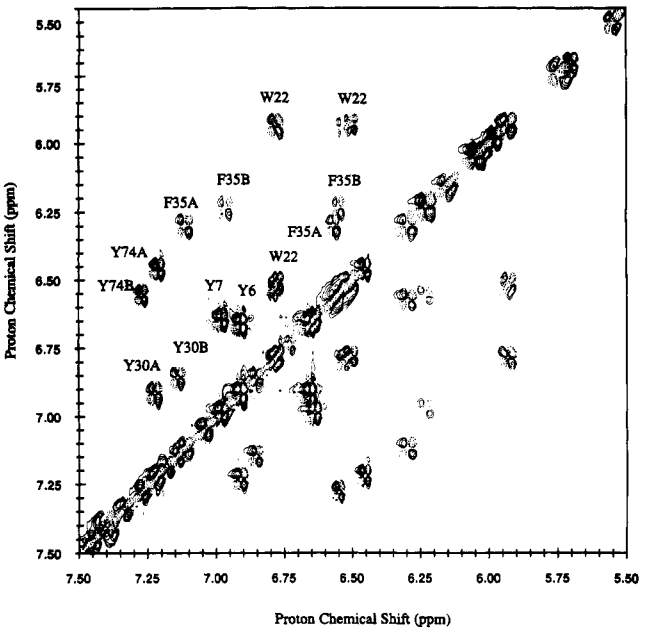

FIGURE 4: Contour plot of the aromatic region of a double-quantum-filtered COSY of rat cytochrome b_5 recorded in D_2O at 40 °C. Large differences between the aromatic resonances of the different conformers are observed for aromatic residues in the heme-binding pocket (e.g., F35 and Y74). A diverse range of effects are observed for residues in the β-sheet. For example, no heterogeneity is observed in the ring resonances of Y6 and Y7, a small degree of heterogeneity is observed for W22, and large conformational shifts are observed for Y30.

Nitrogen-15 resonances are by far the most sensitive to differences in the conformation of the heme. Twenty-nine of the forty-one residues which show differences between the isomers have chemical shift differences of at least 0.1 ppm, and seven differ by more than 0.5 ppm. The majority of the residues in the four helices which surround the heme are affected, and 10 residues (W22, V23, I24, L25, K28, Y30, G51, G52, D53, and A54) of the 22 residues which constitute the β-sheet are affected. The extent of differences between resonances of the two different conformers is surprising, if, in fact, the only difference between the two conformations is a simple back-to-front flip of the heme. This simple rotation would only result in a symmetric exchange of a methyl for a vinyl group, effectively displacing only one heavy atom on each side of the heme. The magnitude of the differences between the conformers is suggestive of more complex changes in the nature of the heme binding.

For some residues the magnitude of ^{15}N-chemical shifts are quite surprising. For example, V23 shows virtually no heterogeneity in the α-carbon proton or amide proton resonances (see Figure 2), and relatively small shifts are observed in side-chain resonances. This is surprising in light of the fact that it is in direct contact with the heme and this residue is the one which is largely responsible for the shift in the equilibrium distribution of conformers (Lee et al., 1990). However, ring-current calculations using the bovine crystal structure as a model indicate that none of the protons on L23 show heme-induced shifts greater than 0.2 ppm (Guiles et al., 1990). Thus, it seems coincidentally that, although the protons on this residue are near the heme, they are also close enough to the magic angle relative to the heme plane to result in small ring-current shifts. This also implies that the differences observed in the ^{15}N chemical shifts between isomers are due to structural differences in the amide bond of V23 in the rat protein.

Table II: Heme Proton Resonance Assignments[a]

assignment	isomer A	isomer B	assignment	isomer A	isomer B
α-meso	9.29	9.48	4-HCα	8.27	8.34
β-meso	9.79	9.77	4-HCβ(trans)	6.05	4.58
γ-meso	9.32	9.34	4-HCβ(cis)	5.96	5.19
δ-meso	9.89	9.76	1-CH_3	3.28	3.52
2-HCα	7.41	7.87	3-CH_3	3.38	2.87
2-HCβ(trans)	5.42	6.23	5-CH_3	3.52	3.64
2-HCβ(cis)	5.06	5.69	8-CH_3	3.66	3.54

[a] All spectra on which these assignments are based, e.g., DQFCOSY, HOHAHA, and NOESY, were recorded at 40 °C, pH 7.0, in 100 mM phosphate buffer. Heme protons are designated according to the nomenclature used in Pochapsky et al. (1990).

Isomer-Specific Assignment Procedures. Approximately 40% of the residues of the protein had proton or ^{15}N resonances which were doubled due to the presence of the two equilibrium orientations of the heme. Deconvolution and assignment of these resonances to specific heme orientations were accomplished by two principal means. The first, and ultimately the only, means by which conformer-specific assignments can be made is on the basis of unique NOESY cross-peaks due to heme proton to protein proton connectivities which directly establish which specific orientation of the heme is in the binding pocket. Our assignments for the heme resonances (see Table II) are in complete agreement with recently published assignments for both equilibrium conformers (Pochapsky et al., 1990) except for minor differences due to differences in the temperatures of acquisition of spectra.

We have assigned more than 60 NOESY cross-peaks between the heme and protein side chains (see Table III). Heme proton to protein proton NOESY cross-peaks fall into three catagories: (1) Connectivities between side chains of residues in the binding pocket and protons on the heme on or near the axis of rotation. This sort of connectivity does not allow conformer-specific assignments. Contacts between the δ-methyl protons of L25 and L46 and the α-meso proton of the heme are an example of this type of connectivity. (2) Connectivities between a side-chain proton and a specific proton of the heme in the A isomer and to its symmetric counterpart in the B isomer (e.g., the γ-methyls of V61 and the β-meso and 5-methyl protons in the A-form and the δ-meso and 8-methyl protons in the B-form are an example of this type of symmetry related connectivity). This sort of connectivity directly establishes conformer identity. (3) The final type of connectivity is not symmetrical in form with respect to the two isomers. For example, the V61 γ-methyl protons show a cross-peak between the heme 1-methyl protons in the B isomer but do not show expected cross-peaks to the 4-vinyl resonances in the A form. Similarly, the L46 δ-methyl protons show cross-peaks to the 3-methyl protons of the heme in both equilibrium orientations which would not necessarily be expected for a symmetric flip given the displacement from the axis of rotation.

This last class of unsymmetrical cross-peaks suggests that additional differences between the two heme orientations. The simplest explanation of these cross-peaks is a 5–10° counterclockwise rotation of the heme about an axis normal to the heme plane passing through the iron facing the heme from the H63 side as has been previsouly suggested (Pochapsky et al., 1990). As indicated above, such shifts in the orientation of the heme might also explain some of the large differences in chemical shift observed between the isomers. Continuous sequential connectivities between residues assigned to a given heme conformation then established the specific conformer assignment for residues not in direct contact with the heme.

Table III: Heme Proton to Protein Proton NOESY Connectivities[a]

	residue												
heme proton	V23	L25	L32	F35	G41	V45	L46	N57	V61	H63	A67	L70	Y74
α-meso	Aγ′	A,Bδδ′					A,Bδ′						
β-meso				Bεζ		Aγγ′			Aγγ′			Bγ	
γ-meso					Aα,α′								
δ-meso				Aεζ		Bγγ′			Bγγ′	Aβ		Aγδ′	
2-HCα		Aδ′					Bδ′						
2-HCβ(trans)							Bδ′						
2-HCβ(cis)		Aδ′				Bγ							
4-HCα													
4-HCβ(trans)				Bζ									Bδε
4-HCβ(cis)													
1-CH_3				Aδεζ				Bβ	Bβγ′			Aγ	Aδε
3-CH_3	Aγγ′	Aδδ′,Bδ′	Bβ′				A,Bδ′						
5-CH_3				Bζ	Aα′	Aγγ′			Aγγ′				
8-CH_3				Aζ		Bγγ′			Bγγ′		Aαβ		

[a] A NOESY peak between a given heme proton and a protein proton of one of the residues in the heme-binding pocket is identified in this table as being observed in isomer A or B followed by the specific proton or protons observed.

Heteronuclear correlation methods provide a second means for corroborating specific conformer assignments. A major advantage in this system is the conformationally independent peak intensity of heteronuclear correlations. With the exception of the short disordered N-terminal sequence, all expected correlations were observed, due principally to the large (90-Hz) one-bond couplings between amide protons and the amide ^{15}N nuclei. As described in more detail above, a major difficulty in our earlier work with proton methods alone on other species variants was the absence of a number of COSY fingerprint peaks due to small $^3J_{N\alpha}$ couplings. Under the conditions under which we performed the NMR experiments (more significantly the temperature at which the sample was equilibrated in the days before the experiment) the distribution of conformers was close to 60/40. This was determined from the intensity data from a set of 13 spin systems which showed clearly resolved correlation peaks for both conformations. The peak intensities indicate a relative abundance of 61.7 ± 2.3% for the A-form and 38.3 ± 2.2% for the B-form. The tight distribution of relative intensities for A and B conformations determined from the integration of correlation peaks suggest that differences between relaxation and exchange rates for a proton on a given residue are not significantly different between conformations. However, despite the uniformity in ^{15}N–proton couplings, we found substantial variation in heteronuclear correlation peak intensities for different residues, presumably due to varying relaxation rates. For a set of 20 well-resolved peaks which we assigned to the sum of contributions from both A- and B-forms, the integrated intensities were on average $(1.19 \pm 0.44) \times 10^7$ (A.U.). The average intensity determined from a set of 20 well-resolved peaks corresponding to the A-form alone was found to be $(0.82 \pm 0.3) \times 10^7$ (69% of the intensity found for peaks corresponding to both isomers). Similarly for a set of 20 well-resolved peaks corresponding to the B-form the average intensity was found to be $(0.57 \pm 0.21) \times 10^7$ (48% of the intensity of peaks corresponding to both isomers). Thus, we found that integration of heteronuclear correlation peaks yielded intensities which were reliable indicators of the particular conformer and statistically provided some corroborative evidence that a given correlation peak did, in fact, contain contributions from both A and B conformations. It is important to note that of the 128 intense peaks in the heteronuclear correlation spectrum only two peaks were not assigned. In addition, no more than four much weaker peaks were observed which we were not able to assign. Presumably, the majority of these unassigned peaks correspond to the five N-terminal residues which we were unable to assign.

Once the majority of the spin systems were established as to the type of amino acid, isomer-specific sequential connectivities were established through combined use of conventional NOESY spectra and NOESY relayed heteronuclear correlation spectra. In many cases near coincidence of resonances in proton spectra alone yielded ambiguities which complicated sequential assignment. However, in most cases such accidental coincidences were easily deconvolved in NOESY relayed heteronuclear correlation spectra due to the noncoincidence of ^{15}N resonance frequencies. For example, as described above, the resonances of V23 in each isomer are nearly coincident for all nuclei except for the amide ^{15}N nuclei. Thus, in the proton NOESY this would be a point of convergence of the connectivity paths which characterize each isomer and would lead to ambiguity in subsequent isomer-specific sequential connectivities. However, because the ^{15}N resonances of the amides of V23 are well resolved, sequence- and isomer-specific assignments determined by ^{15}N-correlated amide connectivities observed in the NOESY relayed heteronuclear correlation spectra allow unambiguous assignment. Similarly, clusters of peaks which were observed in the fingerprint region of the double-quantum-filtered COSY are easily deconvolved and assigned on the basis of ^{15}N-correlated NOESY connectivites. For example, while V4 and E37 have nearly overlapping fingerprint peaks in the DQFCOSY (the amides are within 0.01 ppm), the ^{15}N resonances differ by nearly 10 ppm.

The ease of deconvolution of amide proton coincidences with ^{15}N-correlated NOESY connectivites is illustrated in Figure 5. As shown in the figure, the amide–amide NOESY connectivity paths for helices IV and VI intersect at the amide resonance of D60 of helix IV and the amide resonance of D83 of helix VI due to an accidental coincidence of amide frequencies. However, the connectivity paths in the NOESY relayed heteronuclear correlation spectrum clearly deconvolve this ambiguity through clearcut $^{15}N_i$ to NH_{i+1} connectivities involving the very different ^{15}N chemical shifts of D60 and D83. A complete listing of short-range connectivities, i.e., i to $i + 3$, illustrated schematically in the assignment diagram in Figure 6.

For each of the four helices encasing the heme (e.g., helices II–V) nearly completely separate connectivity paths can be traced in both proton–proton NOESY spectra and NOESY relayed heteronuclear correlation spectra. Figure 7 illustrates parallel NOESY connectivity paths for conformers A and B for helix V. As is illustrated here, in general, the fact that the distribution of ^{15}N resonances is simply different from

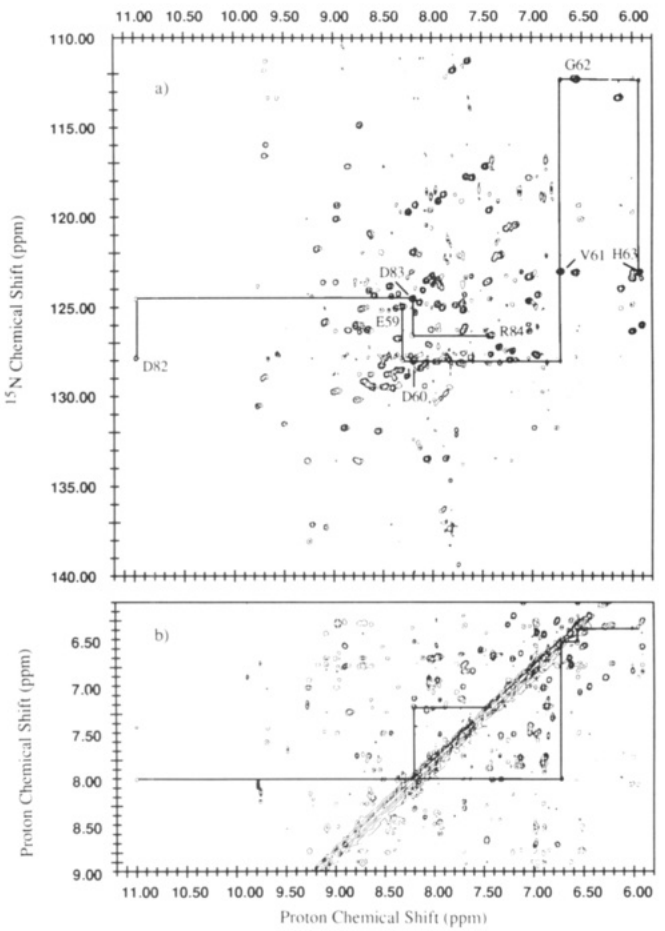

FIGURE 5: A comparison of NOESY connectivity pathways in a NOESY relayed heteronuclear ^{15}N–^{1}H correlation spectrum and a proton–proton NOESY spectrum. Panel a is a contour plot of a NOESY relayed heteronuclear ^{15}N–^{1}H correlation spectrum recorded using the double-DEPT sequence. Note that panel a is of the same region as the ^{15}N–^{1}H correlation plot shown in Figure 1; however, in addition to the direct one-bond correlation peaks observed in Figure 1, there are weaker NOESY relayed peaks present in this region which connect sequential residues in helical segments of the protein. Connectivity paths for two short helical segments (e.g., E59 → H63 of helix IV and D82 → R84 of helix VI) are shown. Note that the amide resonances of D60 and D83 are virtually coincident; however, because the ^{15}N resonances of these two spin systems are quite distinct and the NOESY relays are correlated with the ^{15}N frequencies, ambiguities present in the proton–proton NOESY spectrum can be resolved. Panel b is a contour plot of the amide–amide region of a proton–proton NOESY spectrum. Amide proton connectivity patterns for helix IV are displayed below the diagonal and the connectivity path for helix VI is shown above the diagonal. Note that, unlike the pattern shown in panel a, the paths intersect at the amide frequency of D60 and D83. Note also the sequential amide–amide cross-peak connecting E59 to D60 is too close to the diagonal to be clearly visible. For both the ^{1}H–^{1}H NOESY and the NOESY relayed heteronuclear correlation spectrum experiments the NOESY mixing times of 100 ms were used. Sample conditions and spectrometer settings are identical to those of spectra presented in Figures 1 and 2.

that of proton resonances leads to a different pattern of overlapping cross-peaks, and successful deconvolution of sequence-specific connectivity paths is achieved by parallel examination of NOESY and NOESY relayed heteronuclear correlation spectra. For example, the L70 to S71 amide–amide connectivity in the NOESY spectrum could not have been unambiguously assigned on the basis of the NOESY spectrum alone because of the presence of at least two other NOESY cross-peaks aligned along the L70 amide resonance frequency; however, the ^{15}N-correlated amide–amide NOESY connectivity between S71 and L70 clearly indicates the correct

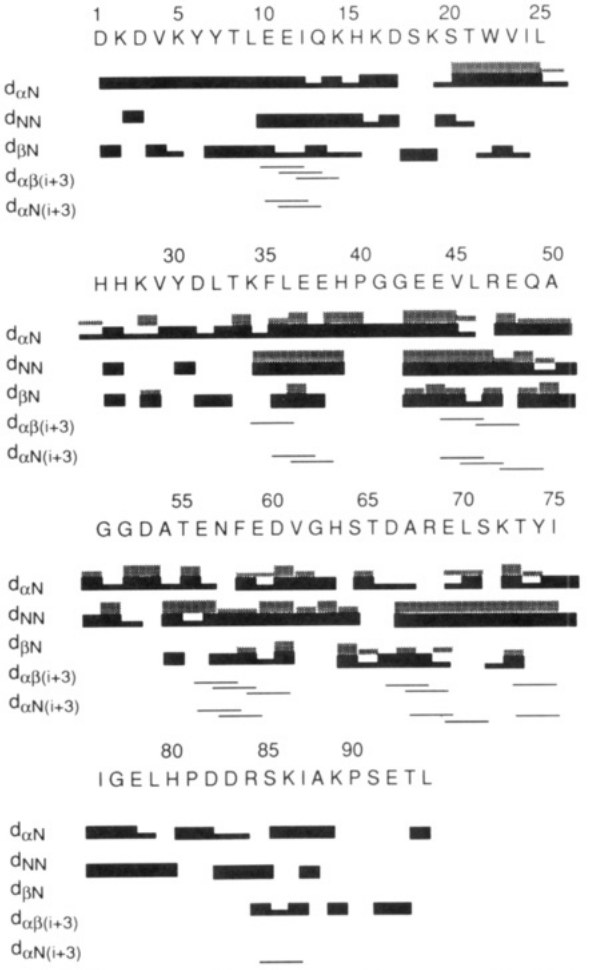

FIGURE 6: A summary of sequence-specific connectivities for both equilibrium forms of rat ferrocytochrome b_5. The solid bars represent connectivities for the A-form. Sequential connectivities for the B-form are indicated by shaded bars above the A-form connectivities. Separate connectivities are observed for the two equilibrium forms for a small region of the β-sheet (e.g., residues 20–25) and for most of the residues in the four helices which form the binding site for the heme. Wide bars indicate strong unambiguous sequential connectivities while narrow bars indicate a peak of lower intensity. Regions which do not show separate and clearly distinguishable connectivities are assumed to be the same for both conformers.

NOESY cross-peak involved in this connectivity pattern. Conversely, the ^{15}N resonances of E69 and L70 in the A isomer are aligned, but their amide proton resonances are well resolved. Generally, the parallel patterns of connectivity involved in each isomer were similar to the single patterns observed in other species variants. Thus, as described above, while direct transfer of resonance assignments was not generally possible, similar patterns of NOESY connectivities observed enabled facile assignment on the basis of our earlier work.

DISCUSSION

The heterogeneity observed in proton and ^{15}N resonance assignments of the rat cytochrome b_5 system is the most extensive among assigned proteins reported to date. In the discussion below, we describe probable origins of this heterogeneity, compare the rat assignments with those of previously assigned species variants, compare our results with conformational heterogeneity observed in other systems, and discuss briefly current issues in the treatment of multiple conformations in the refinement of NMR solution structures.

Origins of Heterogeneity in the Rat Cytochrome b_5 Systems. The level of heterogeneity evident in the NMR spectrum of

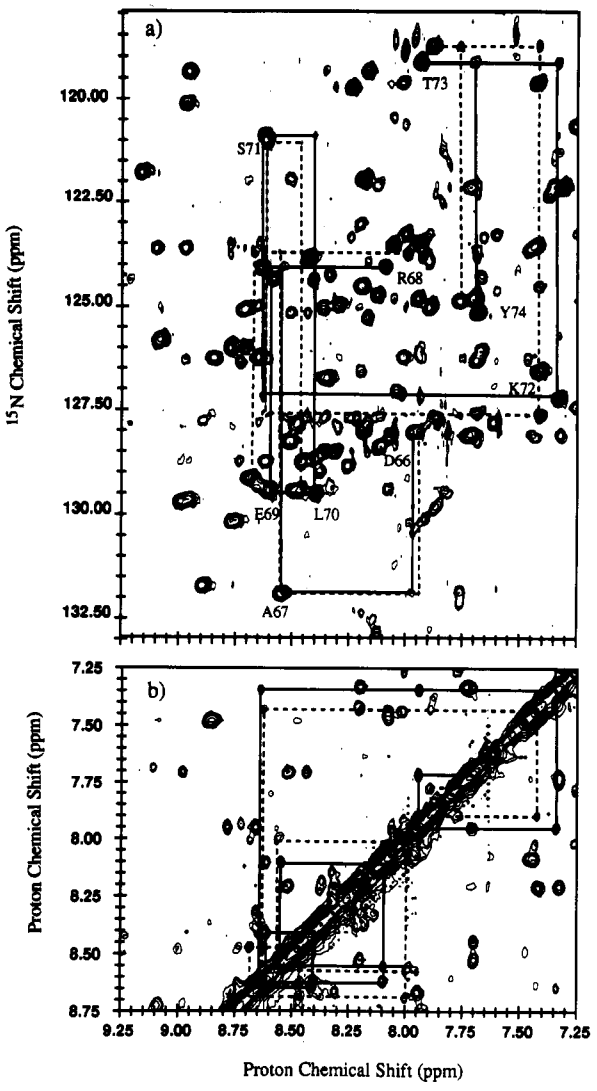

FIGURE 7: A comparison of NOESY connectivity pathways observed for each isomer for helix V. In panels a and b are shown the connectivity pathways for both conformers A and B. The connectivity pathway for the A isomer is indicated with a solid line, while the parallel pathway for the B isomer is indicated with a dashed line. (a) Connectivity pattern in a NOESY relayed heteronuclear ^{15}N–^{1}H correlation spectrum; and (b) the same pattern in a ^{1}H–^{1}H NOESY spectrum. Sample conditions and spectrometer settings are identical to those of Figure 5.

the equilibrium distribution of isomers present in solutions of the rat cytochrome b_5 attests to the extreme sensitivity of chemical shifts to subtle changes in local conformation (e.g., changes in hydrogen bond strengths or the orientation of aromatic rings relative to a given proton). There is now an abundance of evidence confirming the fact that the dominant source of the observed differences in conformation is a 180° flip of the heme about the α,γ-meso axis (Pochapsky et al., 1990; Lee et al., 1990). This flip, itself, would be expected to have little effect on chemical shifts of the residues in the heme-binding pocket considering the high symmetry of the heme moiety. Thus, given the magnitude of observed chemical shift differences between the equilibrium conformations, it appears unlikely that this simple back-to-front flip of the heme is solely responsible for the observed changes. A number of protein proton to heme proton connectivities which are asymmetrical with respect to the 180° rotation indicate that an additional axial rotation of the heme occurs in agreement with the proposal of Pochapsky et al. (1990). A rotation of between 5° and 10° about an axis perpendicular to the heme plane could explain these observed asymmetries in NOE contacts with respect to the 180° rotation of the heme. This additional rotation could also explain the widespread differences in the resonance assignments between the two forms in terms of different ring-current fields experienced by residues surrounding the heme in the two orientations.

A Comparison of Species Variants. Of the species variants that we have assigned to date, the porcine protein has the greatest sequence homology with the rat protein. There are six amino acid differences in the 82 residues which are directly comparable (the tryptic fragment of the bovine and porcine proteins is 16 residues shorter than the rat protein). Perhaps not surprisingly, resonance assignments of the porcine protein also most closely resemble those of the rat protein. Of the 71 amide protons which are directly comparable (sites of mutation, prolines and amides in fast exchange were excluded from the comparison) 23 were within the uncertainty normally quoted for proton resonance assignments (e.g., 0.02 ppm). The rat protein isomer A resonance assignments were used in this analysis. Similarly, for α-carbon proton resonances, 38 out of the 82 directly comparable resonances were within 0.02 ppm. However, only 10 residues had both α-carbon proton and amide proton resonances which were within 0.02 ppm for both proteins. Even among this set of nearly identical resonances between the species variants, direct transfer of assignments was often not possible due to overlapping resonances observed in the rat protein. For example, the amide and α-proton resonances of E37 in the porcine protein are virtually identical to the A isomer of the rat protein (the B isomer resonances are significantly shifted); however, the amide resonances of V4 (not observed in the porcine protein due to fast exchange) is within 0.01 ppm of the E37 amide and hence confounds direct transfer (see Figure 3). The E37 fingerprint resonance is well resolved in the porcine protein. Similarly, the fingerprint peak of F35 which was well resolved in the porcine DQFCOSY (although the amide resonance of Q11 was aligned) appears as a set of overlapping fingerprint peaks (F35A, F35B, and K86) in the rat DQFCOSY. Many such clusters are present in the rat spectra which were absent in other species variants. As we have shown, such complex regions can be assigned through recourse to NOESY and HOHAHA relayed heteronuclear correlation spectra. Thus, while direct transfer of assignments was not generally possible, patterns of connectivity in NOESY and HOHAHA spectra common to all species variants examined often enabled rapid assignment.

Despite the similarities in the rat and porcine spectra, the differences between the resonances of these proteins are far greater than those observed between other species variants. Of the 76 residues which can in principle be directly compared 25 have one or more resonances with shifts greater than 0.1 ppm, and shifts as large as 0.4 ppm are observed. A detailed comparison of porcine and bovine resonance assignments indicates that nearly twice as many comparable protons have resonances which are within 0.02 ppm relative to the number observed within this tolerance between the porcine and rat assignments. For example, of the 74 amides which can be directly compared between porcine and bovine spectra there are 45 that are within this tolerance, compared to 23 out of 71 within this tolerance between the porcine and rat isomer A assignments. Similar ratios of resonances within a tolerance of 0.02 ppm are found for both α- and β-carbon proton resonances. These differences between the similarity of resonance frequencies may simply reflect the number of mutational differences (e.g., three between porcine and bovine compared to eight between procine and rat) or as is suggested

below may reflect differences in the exact binding geometry of the heme found in each species variant.

Curiously enough, the differences between resonance assignments for the equilibrium conformers of the rat protein are nearly as great as the differences between the porcine and bovine species variants. For example, of the 41 residues which exhibit significant conformer heterogeneity 26 of these have amides in the two conformations which differ by more than 0.02 ppm compared to 29 amides which differ by more than 0.02 ppm between porcine and bovine proteins. Variations in α- and β-carbon proton resonances between the conformations of the rat protein are smaller than the differences between bovine and porcine species variants. To this point, discussion of similarities or differences between species variants or conformers has been based on shifts of 0.02 ppm or more, but in fact, shifts between conformers on the order of 0.01–0.02 ppm or 5–10 Hz for an equilibrium mixture of conformations can result in overlap problems in this natural superposition of spectra which seriously complicate interpretation. First, shifts of this magnitude, more common in the α- and β-carbon proton resonances, can result in accidental antiphase cancellation given that the magnitude of the shifts are on the order of typical three-bond coupling constants. And second, such shifts further complicate the already dense regions of COSY and HOHAHA spectra.

A Comparison of Heterogeneity Observed in Other Systems. NMR is among the highest resolution spectroscopic techniques. Recently, an increasing number of studies on proteins have revealed forms of heterogeneity which have gone undetected by other methods of structural or physical characterization. Although NMR is capable of detecting extremely subtle changes in the structure or bonding through the observation of small changes in chemical shifts, the origin of these small differences is often not readily interpretable in terms of a physical model. However, when these small differences are coupled with other chemical, physical, or site-directed mutagenic studies, the origin of these differences can usually be deduced. For example, two-dimensional NMR studies on the calcium binding protein calbindin D_{9K} (Kordel et al., 1990) revealed a doubling of resonances for 22 of the 76 residues (29%). This heterogeneity was found to be due to an equilibrium distribution of cis and trans proline isomers at position 43. Two-dimensional proton and ^{15}N studies of human thioredoxin also revealed substantial heterogeneity: 27 of the 105 residues exhibited two NMR-distinguishable forms. This heterogeneity was found to be due to incomplete posttranscriptional processing of the recombinant protein (Forman-Kay et al., 1990). Similar N-terminal heterogeneity although much less extensive was also detected in interlukin 1β using ^{15}N–^{1}H heteronuclear three-dimensional NMR (Driscoll et al., 1990). In our laboratory studies of wild-type and mutant BPTI proteins have revealed oxidation and deamidation processes which yield widespread NMR-observable heterogeneity. These processes occur spontaneously for conditions under which NMR data are commonly collected (P. A. Kosen, unpublished results, 1991).

Heterogeneity due to multiple conformers in solution has also been found to vary dramatically among species variants in other systems. For example, in studies of acyl-carrier proteins (Kim & Prestegard, 1989; Kim et al., 1990) static heterogeneity between slowly exchanging conformers was observed in the aromatic resonances of spinach acyl-carrier protein. While heterogeneity had not been previously observed for *E. coli* acyl-carrier protein (Kim & Prestegard, 1989), it has been suggested that multiple conformers existed in fast exchange in solution. The observation of static heterogeneity in the spinach species variant provided support for the assertion of rapid exchange in the *E. coli* protein. Presumably amino acid differences between these two species variants resulted in a greater barrier to exchange between conformers, an effect similar to the altered stability of conformers observed between rat cytochrome b_5 and other species variants. The heterogeneity observed in some of the aromatic resonances of spinach acyl-carrier protein is similar but not as marked as that observed in cytochrome b_5.

Issues in the Study of Multiple Conformers in Solution. Heterogeneity poses some interesting challenges to current solution structure methodologies. Recently, a number of computational approaches to static (Kim et al., 1990) and dynamic (Kim & Prestegard, 1989; Torda et al., 1990; Pearlman & Kollman, 1991) heterogeneity have been used in the refinement of solution structures. However, a number of questions regarding the utility of the NMR methods to the elucidation of subtle structural differences between conformers remain unanswered. For a protein which exists as an equilibrium mixture of conformers in solution, can one obtain a sufficient number of constraints to determine the structure of each conformer in solution? Is the resolution of current NMR methods of solution structure refinement sufficient to enable one to discern differences in structure between equilibrium conformers? We believe a structural study of the equilibrium distribution of confomers in the rat cytochrome b_5 protein may in many ways be an ideal test case addressing these issues.

Now that the complete assignment of both equilibrium conformers of the protein is in hand, is a complete structural characterization of both forms of the protein possible with contraints obtainable using NMR methods? Chazin and co-workers (Kordel et al., 1990) have argued that for NOESY cross-peaks between protons with resonance frequencies which are identical or too close to be resolved between conformers, deconvolution of the intensity of that cross-peak into individual conformer intensity contributions is impossible. For proton–proton NOESY methods this is, at least in principle, correct. However, NOESY relayed ^{15}N–proton correlation methods provide a means in many cases of deconvolution of cross-peaks which are coincident in two-dimensional NOESY spectra. Also from our experience with a variety of mutants it seems unlikely that the supposition of Chazin and co-workers is correct. Changes in chemical shift are far more sensitive indicators of subtle changes in protein structure or bonding than are NOESY cross-peak intensities. Our experience with a number of mutants of BPTI is illustrative in this respect (Hurle et al., 1991). In some instances where mutations produced substantial changes in chemical shifts relative to wild-type resonances, not only in the region of the mutation but often far removed, no differences or at most differences near the resolution limit of the method between the NMR solution structures could be discerned. For the case of cytochrome b_5 it is clear that where one expects to observe differences in the protein structure in order to accommodate the different orientations of the heme, large differences in the chemical shifts of residues in each conformer exist. For regions of the protein which are more remote from the heme, protein proton chemical shifts are identical for the two conformers and we would not expect to observe differences.

In summary, our observations support previous suggestions (Pochapsky et al., 1990) that an additional axial rotation of the heme occurs in an apparently rigid hydrophobic binding pocket. The dominant effect of this additional 5–10° rotation

would be a slight realignment of the imidazole planes of the axial histidines in one conformer relative to the other. Such axial ligand plane realignments can theoretically yield changes in midpoint potential on the order of 50 mV (Walker et al., 1986). In fact, such a realignment has been suggested to be the origin of the observed difference in midpoint potentials (Walker et al., 1988). However, it is also possible that the midpoint potential is partially modulated by other more subtle protein–heme interactions which are not obvious at the present level of analysis.

ACKNOWLEDGMENT

We thank Dr. Brad Gibson and the UCSF mass spectrometry laboratory for performing and interpreting the solvent electrospray mass spectrometry on the labeled and unlabeled proteins. We thank Dr. Steve Sligar for providing the puc13 plasmid containing the synthetic gene coding rat cytochrome b_5. We thank Dr. Richard Shand for providing the host strain of *E. coli* (NCM 533) which greatly enhanced the expression yield in minimal media.

REFERENCES

Basus, V. J. (1984) *J. Magn. Reson. 60*, 138–142.
Bax, A. (1989) *Annu. Rev. Biochem. 58*, 223–256.
Bax, A., & Davis, D. G. (1985) *J. Magn. Reson. 65*, 355–360.
Bax, A., Griffey, R. H., & Hawkins, B. L. (1983) *J. Magn. Reson. 55*, 301–315.
Beratan, D. N., Onuchic, J. N., & Hopfield, J. J. (1990a) *J. Chem. Phys. 86*, 4488–4498.
Beratan, D. N., Onuchic, J. N., Betts, J. N., Bowler, B. E., & Gray, H. B. (1990b) *J. Am. Chem. Soc. 112*, 7915–7921.
Billeter, M., Braun, W., & Wüthrich, K. (1982) *J. Mol. Biol. 155*, 321–346.
Detlefsen, D. J., Thanabal, V., Pecoraro, V. L., & Wagner, G. (1990) *Biochemistry 29*, 9377–9386.
Detlefsen, D. J., Thanabal, V., Pecoraro, V. L., & Wagner, G. (1991) *Biochemistry 30*, 9040–9046.
Driscoll, P. C., Clore, M., Marion, D., Wingfield, P. T., & Gronenborn, A. M. (1990) *Biochemistry 29*, 3542–3556.
Feng, Y., Roder, H., Englander, S. W., Wand, A. J., & Di Stefano, D. L. (1989) *Biochemistry 28*, 195–203.
Forman-Kay, J. D., Gronenborn, A. M., Kay, L. E., Wingfield, P. T., & Clore, G. M. (1990) *Biochemistry 29*, 1566–1572.
Gooley, P. R., Caffrey, M. S., Cusanovich, M. A., & Mackenzie, N. E. (1990) *Biochemistry 29*, 2278–2290.
Gray, H. B., & Malmstrom, B. G. (1989) *Biochemistry 28*, 7499–7505.
Griffey, R. H., & Redfield, A. G. (1987) *Q. Rev. Biophys. 19*, 51–82.
Gronenborn, A. M., Bax, A., Wingfield, P. T., & Clore, G. M. (1989) *FEBS Lett. 243*, 93–98.
Guiles, R. D., Altman, J., Lipka, J. J., Kuntz, I. D., & Waskell, L. A. (1990) *Biochemistry 29*, 1276–1279.
Hurle, M. R., Eads, C. D., Pearlman, D. A., Seibel, G. L., Thomason, J., Kosen, P. A., Kollman, P., Anderson, S., & Kuntz, I. D. (1992) *Protein Sci. 1*, 91–106.
Keller, R. M., & Wüthrich, K. (1980) *Biochim. Biophys. Acta 621*, 204–217.
Kim, Y., & Prestegard, J. H. (1989) *Biochemistry 28*, 8792–8797.
Kim, Y., Ohlrogge, J. B., & Prestegard, J. H. (1990) *Biochem. Pharmacol. 40*, 7–13.
Kordel, J., Forsen, S., Drakenberg, T., & Chazin, W. J. (1990) *Biochemistry 29*, 4400–4409.
Lee, K.-B., La Mar, G. N., Kehres, L. A., Fujinari, E. M., Smith, K. M., Pochapsky, T. C., & Sligar, S. G. (1990) *Biochemistry 29*, 9623–9631.
Mathews, F. S., Levine, M., & Argos, P. (1972) *J. Mol. Biol. 64*, 449–464.
Mayo, S. L., Ellis, W. R., Crutchley, R. J., & Gray, H. B. (1986) *Science 233*, 948–952.
McIntosh, L. P., Griffey, R. H., Muchmore, D. C., Nielson, C. P., Redfield, A. G., & Dalhquist, F. J. (1987) *Proc. Natl. Acad. Sci. U.S.A. 83*, 9443–9447.
Ng, S., Smith, M. B., Smith, H. T., & Millet, F. (1977) *Biochemistry 16*, 4975–4978.
Nirmala, N. R., & Wagner, G. (1988) *J. Am. Chem. Soc. 110*, 7557–7558.
Pearlman, D. A., & Kollman, P. A. (1991) *J. Mol. Biol. 220*, 457–479.
Pearson, G. A. (1977) *J. Magn. Reson. 27*, 265–272.
Piantini, O. W., Sørensen, O. W., & Ernst, R. R. (1982) *J. Am. Chem. Soc. 104*, 6800–6801.
Pochapsky, T. C., Sligar, S. G., McLachlan, S. J., & LaMar, G. N. (1990) *J. Am. Chem. Soc. 112*, 5258–5263.
Poulos, T. L., & Kraut, J. (1980) *J. Biol. Chem. 255*, 10322–10330.
Poulos, T. L., & Mauk, A. G. (1983) *J. Biol. Chem. 258*, 7369–7373.
Poulos, T. L., Sheriff, S., & Howard, A. J. (1987) *J. Biol. Chem. 262*, 13881–13884.
Redfield, A. G., & Kunz, S. D. (1975) *J. Magn. Reson. 19*, 250–254.
Rodgers, K. K., & Sligar, S. G. (1991) *J. Mol. Biol. 221*, 1453–1460.
Rodgers, K. K., Pochapsky, T. C., & Sligar, S. G. (1988) *Science 240*, 1657–1659.
Salemme, F. R. (1976) *J. Mol. Biol. 102*, 563–568.
Scott, R. A., Mauk, A. G., & Gray, H. B. (1985) *J. Chem. Educ. 62*, 933–938.
Shaka, A. J., & Freeman, R. (1983) *J. Magn. Reson. 51*, 169–173.
Shaka, A. J., Keeler, J., Frenkiel, T. A., & Freeman, R. (1983) *J. Magn. Reson. 52*, 335–338.
Shand, R. f., Meircke, L. J. W., Mitra, A. K., Fong, S. K., Stroud, R. M., & Betlach, M. C. (1991) *Biochemistry 30*, 3082–3091.
States, D. J., Haberkorn, R. A., & Ruben, D. J. (1982) *J. Magn. Reson. 48*, 286–292.
Strittmatter, P., & Velick, S. F. (1956) *J. Biol. Chem. 221*, 253–264.
Torchia, D. A., Sparks, S. W., & Bax, A. (1989) *Biochemistry 28*, 5509–5524.
Torda, A. E., Scheek, R. M., & van Gunsteren, W. F. (1990) *J. Mol. Biol. 214*, 223–235.
Veitch, N. C., Whitford, D., & Williams, R. J. P. (1990) *FEBS Lett. 269*, 297–304.
von Bodman, S. B., Schulder, M. A., Jollie, D. R., & Sligar, S. G. (1986) *Proc. Natl. Acad. Sci. U.S.A. 83*, 9443–9447.
Walker, F. A., Huynh, B. H., Scheidt, W. R., & Osvath, S. R. (1986) *J. Am. Chem. Soc. 108*, 5288–5297.
Walker, F. A., Emrick, D., Rivera, J. E., Hanquet, B. J., & Buttlaire, D. H. (1988) *J. Am. Chem. Soc. 110*, 6234–6240.
Wand, A. J., Di Stefano, D. L., Feng, Y., Roder, H., & Englander, S. W. (1989) *Biochemistry 28*, 186–194.
Wendoloski, J. J., Mathew, J. B., Weber, P. C., & Salemme, F. R. (1987) *Science 238*, 794–797.
Wüthrich, K., Billeter, M., & Braun, W. (1984) *J. Mol. Biol. 180*, 715–740.

Registry No. Cytochrome b_5, 9035-39-6; heme, 14875-96-8.